RESEARCH ARTICLE

Human Mutation

OFFICIAL JOURNAL HGVS HUMAN GENOME VARIATION SOCIETY www.hgvs.org

Functional Characterization and Rescue of a Deep Intronic Mutation in *OCRL* Gene Responsible for Lowe Syndrome

John Rendu,[1,2,3] Rodrick Montjean,[4,11] Charles Coutton,[5] Mohnish Suri,[6] Gaetan Chicanne,[7,9] Anne Petiot,[1,2] Julie Brocard,[1,2] Didier Grunwald,[1,2] France Pietri Rouxel,[8,10] Bernard Payrastre,[7,9] Joel Lunardi,[1,2,3] Olivier Dorseuil,[4,11] Isabelle Marty,[1,2] and Julien Fauré[1,2,3]*

[1]*Cellular Myology and Pathology, INSERM, U1216, Grenoble, France;* [2]*Grenoble Institut of Neurosciences, Université Grenoble Alpes, France;* [3]*Biochimie Génétique et Moléculaire, CHU Grenoble Alpes, France;* [4]*Institut Cochin, INSERM U1016, Paris, France;* [5]*Laboratoire de Génétique Chromosomique, CHU Grenoble Alpes, France;* [6]*Nottingham Clinical Genetics Service, Nottingham University Hospitals NHS Trust, Nottingham, United Kingdom;* [7]*I2MC, INSERM U1048, Toulouse, France;* [8]*Research Center of Myology, INSERM UMRS974, Paris, France;* [9]*Laboratoire d'Hématologie, CHU de Toulouse, France;* [10]*CNRS FRE3617, UPMC, Paris, France;* [11]*CNRS UMR8104, Université Paris Descartes, Paris, France*

Communicated by Garry Cutting

Received 26 May 2016; accepted revised manuscript 13 October 2016.
Published online 28 October 2016 in Wiley Online Library (www.wiley.com/humanmutation). DOI: 10.1002/humu.23139

ABSTRACT: **Dent-2 disease and Lowe syndrome are two pathologies caused by mutations in inositol polyphosphate 5-phosphatase OCRL gene. Both conditions share proximal tubulopathy evolving to chronic kidney failure. Lowe syndrome is in addition defined by a bilateral congenital cataract, intellectual disability, and hypotonia. The pathology evolves in two decades to a severe condition with renal complications and a fatal issue. We describe here a proof of principle for a targeted gene therapy on a mutation of the OCRL gene that is associated with Lowe syndrome. The affected patient bears a deep intronic mutation inducing a pseudo-exon inclusion in the mRNA, leading to a OCRL-1 protein loss. An exon-skipping strategy was designed to correct the effect of the mutation in cultured cells. We show that a recombinant U7-modified small RNA efficiently triggered the restoration of normal OCRL expression at mRNA and protein levels in patient's fibroblasts. Moreover, the PI(4,5)P2 accumulation and cellular alterations that are hallmark of OCRL-1 dysfunction were also rescued. Altogether, we provide evidence that the restoration of OCRL-1 protein, even at a reduced level, through RNA-based therapy represents a potential therapeutic approach for patients with OCRL splice mutations.**
Hum Mutat 38:152–159, 2017. © 2016 Wiley Periodicals, Inc.

KEY WORDS: exon skipping; Lowe syndrome; OCRL; U7

Introduction

Mutations in the *OCRL* gene (MIM# 300535) are associated with two X-linked recessive pathologies altering kidney function: Dent-2 disease (MIM# 300555) and oculocerebrorenal syndrome of Lowe (MIM# 309000) [Nussbaum et al., 1997; Hoopes et al., 2005]. Dent disease is a renal tubulopathy characterized by low molecular weight proteinuria, hypercalciuria, and progressive renal failure. Oculocerebrorenal syndrome of Lowe is a rare and severe disorder characterized by a triad of symptoms in the eye, the kidney, and in the central nervous system [Lowe et al., 1952]. Affected boys present with congenital bilateral cataracts frequently associated with other ocular signs such as glaucoma, microphthalmia, and corneal keloid formation. Other cardinal early signs are neonatal hypotonia and areflexia [Loi, 2006]. A renal proximal tubulopathy is characteristic of the pathology, although the onset of this dysfunction may vary between patients. Invariably, low molecular weight proteinuria is reported, frequently in association with aminoaciduria, hypercalciuria, and bicarbonaturia [Cho et al., 2008]. A progressive glomerula dysfunction finally leads to renal failure. The majority of patients suffering from Lowe syndrome also show delays in cognitive development and/or specific behavioral troubles [Loi, 2006].

The *OCRL* gene, localized on chromosome Xq24.26, is expressed as a mRNA sequence of 23 exons, spliced in a specific form in the brain that includes the alternative 18a exon [Nussbaum et al., 1997; Vicinanza et al., 2011]. Nonsense mutations, frameshifts, genomic deletions, and splice mutations leading to the apparition of premature STOP codons represent two-third of the more than 200 mutations identified in *OCRL* [Hichri et al., 2011; Recker et al., 2015]. Missense mutations are also detected all along the *OCRL* coding sequence, most of them clustering in exons 9 to 15 that encode the 5-phosphatase domain. Overall, the reduction of the OCRL-1 phosphoinositide phosphatase activity, either by loss of protein expression or perturbation of its enzymatic site, clearly underlies the pathophysiology of oculocerebrorenal syndrome of Lowe.

The *OCRL* gene encodes a type II inositol polyphosphate 5-phosphatase hydrolyzing preferentially phosphatidylinositol 4,5-bisphosphate (PI(4,5)P2) [Attree et al., 1992; Zhang et al., 1998; Lowe, 2005] and participating to the balance of phosphoinositides species in cells [Di Paolo and De Camilli, 2006]. In addition to its 5-phosphatase activity, OCRL-1 is able to interact with several partners mainly involved in intracellular trafficking [Faucherre et al., 2003, Di Paolo and De Camilli, 2006, McCrea et al., 2008]. Cells lacking OCRL-1 function accumulate PI(4,5)P2 [Zhang et al., 1998;

Additional Supporting Information may be found in the online version of this article.

Contract grant sponsor: Association du Syndrome de Lowe.

*Correspondence to: Julien Fauré, Laboratoire de Biochimie Génétique et Moléculaire, Centre Hospitalier Universitaire de Grenoble 217X, Grenoble Cedex 38043, France. E-mail: jfaure1@chu-grenoble.fr

Faucherre et al., 2003; Wenk et al., 2003] and notably show dysfunction in actin polymerization [Suchy and Nussbaum, 2002], phagocytosis and endocytosis [Erdmann et al., 2007], development of polarity [Grieve et al., 2011], ciliogenesis [Coon et al., 2012; Madhivanan et al., 2015], and cytokinesis [Dambournet et al., 2011]. It has been proposed that a default in the traffic of the LRP2 (megalin) receptor, responsible for the uptake of low molecular weight proteins in the proximal tubule, could account for a part of the renal phenotype of Lowe and Dent diseases [Vicinanza et al., 2011].

We have previously reported the c.238+4701 A>G mutation of *OCRL* in a patient suffering from Lowe syndrome [Hichri et al., 2011]. We show here that this deep intronic mutation leads to a drastic decrease in *OCRL* expression due to the insertion of intronic sequences in *OCRL* mRNA. The recent advances in RNA manipulation have led to the development of potential gene therapies for such mutations inducing incorporation of intronic sequences in the mRNA (also called pseudo-exon insertion). The exon-skipping strategy relies on the delivery of antisense oligonucleotides hybridizing on the splice regulatory sequences of the pseudo-exon and able to block its incorporation into the nascent mRNA [Dominski and Kole, 1993]. We show here the design of an efficient exon-skipping strategy able to restore significant levels of *OCRL* mRNA, protein, and enzymatic activity in cells of this patient. We also show the rescue of cellular dysfunctions correlated to the *OCRL* mutation, suggesting that this personal therapeutic approach could lead to a possible treatment for *OCRL*-related diseases.

Materials and Methods

Gene Nomenclature Information

The *OCRL* sequence used in this work is accessible as NCBI RefSeq NM_000276.3. Nucleotide numbering was based on the cDNA sequence (#NM_000276.3) with +1 corresponding to the A of the ATG initiation codon of translation (exon 1) in the reference sequence.

Antibodies and Plasmids

The primary antibodies used for Western blot and immunofluorescence were as follows: rabbit anti OCRL-1 serum [Hichri et al., 2011], mouse monoclonal anti beta-tubulin (TUB2.1; Sigma, Saint Louis, Missouri), rabbit polyclonal anti gamma-tubulin (Sigma), mouse monoclonal antibody against acetylated alpha-tubulin (611b1; Sigma), mouse monoclonal anti alpha-actinin (Sigma), mouse monoclonal anti-PI(4,5)P2 (2C11; Santa Cruz Biotechnologies, Dallas, Texas), and rabbit polyclonal clonal anti-SNX9 (Sigma). Lentiviral vectors were generated by triple transfection of HEK293T cells with the following plasmids from the Addgene repository: PsPAX2, pCMV-VSVG, and pWPXLd modified to express the transgene.

Cell Cultures

Primary skin fibroblasts from a healthy donor and the patient bearing the *OCRL* c.238+4701 A>G; p.Ser80_Gly81ins22*4 mutation were cultured as already described [Hichri et al., 2011]. Investigations on patient material were performed after signature of an informed consent by the patients according to French regulation.

cDNA Analysis

Primary cells were lyzed in TRIzol reagent (Invitrogen, Life Technologies SAS, Saint Aubin, France). After total RNA extraction, cDNA was synthesized, amplified, and sequenced as previously described [Hichri et al., 2011; Rendu et al., 2013]. Reverse transcription followed by multiplex ligation probe amplification (RT-MLPA) was performed with gene exon-specific MLPA probes into *OCRL* exons 20 and 21, exon 4, and the pseudo-exon, into *INPP5B* (NM_005540.2) exons 19 and 20 and into the housekeeping gene *ARID1A* (NM_006015.4) (used for normalization) exon 6 and 7 (Supp. Table S1) [Coutton et al., 2013]. Quantification was realized after an area peak surface analysis with the Genemapper software.

Quantitative Western Blot Analysis

The amount of OCRL-1 present in fibroblast sample was determined by quantitative Western blot analysis using antibodies directed against OCRL-1 and normalized to the amount of beta-tubulin as described previously [Hichri et al., 2011]. Signals were acquired on a Chemidoc-XRS apparatus (Biorad, Hercules, California) and quantified using the Quantity One software (Biorad).

U7 snRNA Lentiviral Vectors and Transduction

The U7_SKIP and control constructs were derived from the previously described U7SmOPT [Goyenvalle et al., 2009; Goyenvalle and Davies, 2011; Rendu et al., 2013]. The sequence of U7SmOPT targeting the histone pre-mRNA was replaced by the specific antisense sequences (Supp. Table S1) by standard cloning procedures. The antisense was chosen after having tested the effect of four sequences encompassing exon 4b splice sites (data not shown). The U7_CTRL and U7_SKIP coding sequences were subcloned into the pWPXLD plasmid. Cultured fibroblasts were transduced with the lentiviral particles (at a multiplicity of infection of 100) for 8 hr, amplified, and split into several dishes to perform RNA, protein, and immunofluorescence studies.

Image Analysis

Immunolabeling of alpha-actinin and PI(4,5)P2 in fibroblasts has been performed as previously described [Montjean et al., 2014]. Briefly, alpha-actinin staining was investigated on cells fixed with methanol and immununolabeled with specific antibody raised against alpha-actinin. The various fibroblast cultures were scored for pattern of alpha-actinin in three independent blind experiments, with more than 100 cells from each condition per experiment. Cell preparations were observed under a Leica epifluorescence microscope coupled to a Coolsnap Cf camera (Photometrics, Tucson, Arizona). For PI(4,5)P2 staining, cells were fixed in 4% formaldehyde, 0.01% Triton X-100, and 0.2% glutaraldehyde, blocked and permeabilized with a solution containing 5% normal goat serum, 50 mM NH_4Cl, and 0.5% saponin and incubated with the 2C11 antibody. PI(4,5)P2 signals for each cell were quantified using ImageJ software, in three independent blind experiments, with more than 15 cells of each patient per experiment. For SNX9 staining, cells were fixed with 4% paraformaldehyde in PBS and incubated 15 min in NH4Cl 50 mM. Permeabilization was realized with 0.1% Triton in PBS containing 0.5% BSA and 2% of goat serum for 45 min, and cells were incubated with the anti-SNX9 antibody for 3 hr at room temperature. Pictures were taken with a Zeiss Axiovert microscope and fibroblasts were classified for SNX9 pattern.

For the ciliogenesis assay, fibroblasts were starved for 42 hr in serum-free medium. Cells were then fixed with methanol at –20°C and processed for immunolabeling. They were analyzed using a

Leica SPE confocal laser scanning microscope (Leica Microsystemes SAS, Nanterre, France) with an x63 oil objective. The cilia length was determined by traces going from the centrosome to the end of the cilium using ImageJ's segmented line tool (version 1.44i, NIH, USA) as previously described [Coon et al., 2012].

Statistics

Statistics were performed using ANOVA followed by Bonferroni *t*-test for multiple comparisons, on Prism 4.0 software (GraphPad, San Diego, CA), with n = number of cells in at least three different experiments.

Results

Clinical and Genetic Case Report

The proband is the second child of healthy unrelated parents with no medical history of early-onset cataracts or renal disease. He was born at term; the motor milestones were normally acquired but his speech and language development was delayed. Short stature was noticed at the age of 3 years and small bilateral cataracts were observed during a routine pre-school vision screening test. A diagnosis of acute and chronic renal failure was made during hospitalization at the age of 5 years after a 3-week episode of vomiting, headaches, and weight loss.

The combination of congenital cataracts, mild speech and language delay, short stature, and renal problems raised concerns about a possible underlying diagnosis of Lowe syndrome. No mutation was found in the DNA of the patient after sequencing of the entire coding region of the *OCRL* gene. Cultured fibroblasts were obtained from a skin biopsy, and *OCRL* mRNA was analyzed by RT-PCR and sequencing. A 66-bp insertion between exon 4 and 5 of *OCRL* transcript was revealed without any other nucleotide variation (Fig. 1A). The inserted sequence was identified as a region of the intron 4 that was further sequenced on genomic DNA, and the c.238+4701 A>G transition was found in intron 4 of the *OCRL* gene. The consequence of this deep intronic mutation was the creation of a donor splice site at the c.238+4701 position, which activated an upstream cryptic acceptor site leading to the incorporation of 66 bp of intron 4 in the mRNA, referred to as pseudo-exon 4b (Fig. 1A). The PCR amplification of exon 1–5 of *OCRL* in the patient cDNA resulted in a single fragment of higher molecular weight and of reduced intensity compared with control (Fig. 1B). We concluded that sites activated by the c.238+4701 A>G mutation were efficiently used during *OCRL* mRNA splicing, and that in patient cells most of *OCRL* mRNA molecules contained pseudo-exon 4b. An in-frame STOP codon is present within the pseudo-exon 4b sequence (Supp. Fig. S1) and the OCRL-1 protein in fibroblasts of the patient was accordingly undetectable by Western blot (Fig. 1C). The conclusion of this molecular diagnosis was therefore that a severe decrease in the amount of OCRL-1 protein was responsible for Lowe syndrome, arising from the c.238+4701 A>G; p.Ser80_Gly81ins22*4 mutation. Further, familial genetic analysis confirmed that the patient's mother carried the mutation at the heterozygous state.

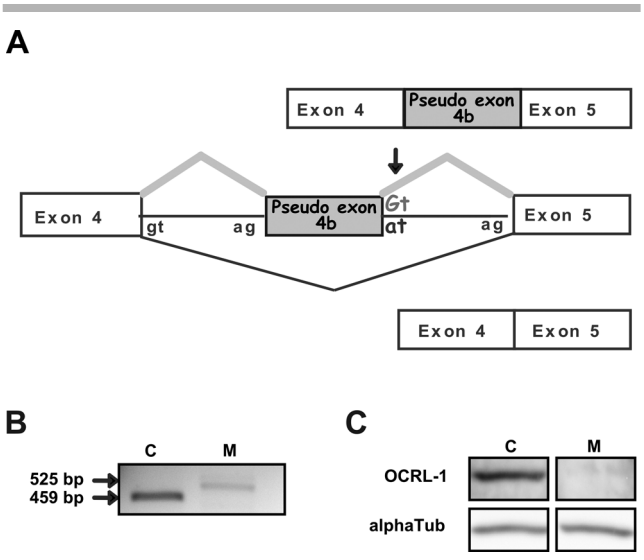

Figure 1. Detection and consequence of the c.238+4701 A>G; p.Ser80_Gly81ins22*4 *OCRL* mutation. **A**: Scheme of splicing events in the C (bottom) or mutated (top) *OCRL* transcripts. The c.238+4701 A>G transition (indicated by a gray arrow) creates a GT donor site and activates a cryptic upstream AG acceptor site leading to 66 bp intronic insertion between exon 4 and 5 of *OCRL*. Mutation numbering was based on the cDNA sequence (#NM_000276.3) wih +1 corresponding to the A of the ATG initiation codon of translation (exon 1) in the reference sequence. **B**: Electrophoresis of RT-PCR product of control (C) or patient (M) cells amplifying exons 1–5. Theoretical product sizes are indicated on the left, according to PCR primers localization. **C**: Western blot analysis of proteins extracted from control (C) or patient (M) primary fibroblasts blotted with either anti-OCRL-1 serum or anti-tubulin antibodies.

U7snRNA-Induced Skipping of Pseudo-Exon 4b

The manipulation of mRNA composition by an antisense oligonucleotide has been proved to be efficient in correcting some genetic defects in vitro [Cavalieri et al., 2012; Rendu et al., 2013; Touznik et al., 2014; Veltrop and Aartsma-Rus, 2014], and in vivo, and is now envisaged for clinical trials in patients. We reasoned that by hindering recognition of the splice sites activated by the c.238 + 4701 A > G mutation, we could force the skipping of this additional exon and induce a partial restoration of normal *OCRL* mRNA in cells of this patient with Lowe syndrome. A U7-modified snRNA [Goyenvalle et al., 2004] containing a 30-bp antisense sequence (Supp. Table S1) targeting splicing regulatory element of pseudo-exon 4b (U7_SKIP) as well as a control U7 snRNA containing a nonrelevant antisense sequence (U7_CTRL) were generated. Lentiviral vectors encoding both U7-modified snRNA were produced. Fibroblasts of the patient were transduced with each lentiviral vector and the inclusion of pseudo-exon 4b in *OCRL* transcripts was first analyzed by RT-PCR. Figure 2A shows that expression of U7_SKIP induced a restoration of the normal *OCRL* mRNA together with a strong reduction in the mutated mRNA. To precisely evaluate these effects, we next used RT-MLPA, a quantitative technique effective with sample with low amount of transcript [Li et al., 2014]. Quantifications of RT-MLPA profiles (Supp. Fig. S2) indicated that patient cells expressing U7_SKIP had a 79% reduction in mutated *OCRL* mRNA (Fig. 2B), showing the efficiency of the exon-skipping strategy. The total *OCRL* mRNA level was also quantified with probes detecting both mutated and normal forms of the transcript. In patient's fibroblasts, total *OCRL* mRNA level was reduced at 28% (±7%) of a control (Fig. 2C) showing that the insertion of pseudo-exon 4b probably induced a degradation of the mRNA. The expression of the U7_SKIP construct triggered a restoration of total *OCRL* mRNA up to 52% (±4%) of a control (Fig. 2C). We concluded that the use of an exon-skipping strategy via U7 snRNA expression in fibroblasts of the patient efficiently inhibited pseudo-exon 4b incorporation in *OCRL* mRNA. Moreover, hindering pseudo-exon 4b incorporation

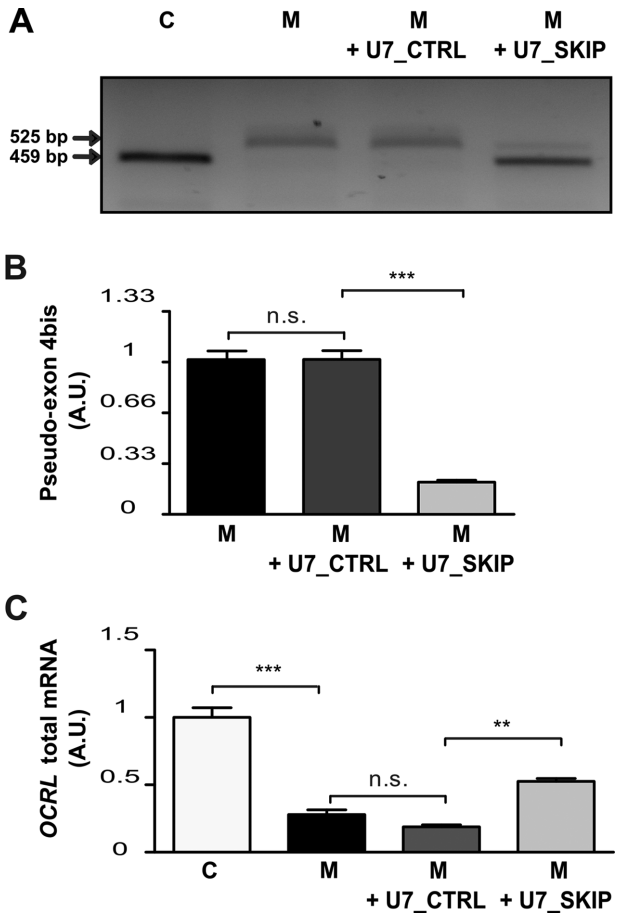

Figure 2. Correction of *OCRL* mRNA by exon-skipping strategy. **A**: Electrophoresis of RT-PCR product with primers amplifying exons 1–5 of *OCRL* of control (C) or patient (M) fibroblasts, or patient fibroblasts transduced with lentiviral vector expressing either the U7_CTRL or U7_SKIP construct. **B**: Histograms represent the average ±SEM of the specific signal for pseudo-exon 4b in RT-MLPA in patient (M) fibroblasts, or patient fibroblasts transduced with lentiviral vector expressing either the U7_CTRL or U7_SKIP construct. **C**: Histograms represent the average ±SEM of the signal detecting the total amount of *OCRL* mRNA in RT-MLPA in control (C) or patient (M) fibroblasts, or patient fibroblasts transduced with lentiviral vector expressing the U7_CTRL or U7_SKIP construct. ANOVA test, $^{***}P < 0.001$, $^{**}P < 0.01$. n.s., nonsignificant; *n*, six experiments.

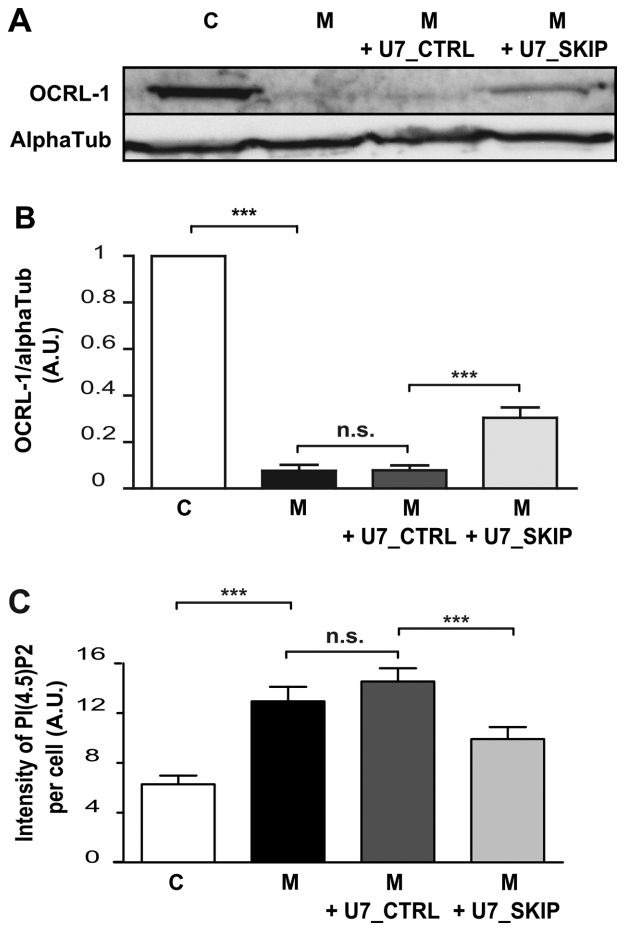

Figure 3. Restoration of functional OCRL-1 protein after exon skipping. **A**: Western blot analysis of proteins extracted from control (C) or patient (M) fibroblasts, or patient fibroblasts transduced with lentiviral vector expressing either the U7_CTRL or U7_SKIP construct, blotted with anti-OCRL-1 or anti-tubulin antibodies. **B**: Quantification of the OCRL-1 signal relatively to tubulin on Western blot analysis as described in **A**. *n* , five experiments. **C**: Histograms represent the average ± SEM PI(4,5)P2 signal detected in immunofluorescence in control (C), patient (M) fibroblasts, or patient fibroblasts transduced with lentiviral vector expressing the U7_CTRL or U7_SKIP construct. *n*, with at least 60 cells of each sample examined. ANOVA test, $^{*}P < 0.05$; $^{***}P < 0.001$; n.s., nonsignificant.

was accompanied by a restoration of *OCRL* mRNA, suggesting that OCRL-1 protein and activity could be restored in treated cells.

Skipping of the Pseudo-Exon 4b Restores OCRL-1 Protein and Phosphatase Activity

We next evaluated the levels the OCRL-1 protein and function after treatment with U7_SKIP. Proteins were extracted from fibroblasts of the patient expressing U7_SKIP and a Western blot analysis showed a significant increase in the level of OCRL-1 protein (Fig. 3A), reaching 30% (±4%) of control fibroblasts (Fig. 3B; $P < 0.001$). As no other variation was found in the *OCRL* sequence in this patient, the restored protein could be considered as functional. This was demonstrated by showing that OCRL-1 immunoprecipitated from fibroblasts lysates after U7_SKIP treatment efficiently transformed in vitro fluorescent PI(4,5)P2 into fluorescent PI4P (Supp. Fig. S3).

We had previously shown that PI(4,5)P2 levels quantified by immunolabeling were significantly elevated in Lowe patient cells [Montjean et al., 2014]. We next investigated whether the restoration of the OCRL-1 protein was able to restore a global PI(4,5)P2 hydrolysis capacity in treated cells (Fig. 3C). As expected, due to the loss of OCRL-1 function, cells from the patient had a PI(4,5)P2 labeling intensity that was much higher (12.9 A.U. ±1.1) than the intensity detected in control cells (6.3 A.U. ±0.7). This PI(4,5)P2 accumulation was reduced by 34% (9.9 A.U. ± 1) after U7_SKIP treatment, whereas it was unchanged when U7_CTRL was used. The *INPP5B* gene is a paralog of *OCRL* reported to compensate *OCRL* loss in animal models [Bernard and Nussbaum, 2010; Bothwell et al., 2010; Luo et al., 2013]. To exclude a compensatory induction of *INPP5B* as an explanation of U7_SKIP effect, we quantified its mRNA levels in our experiments. *INPP5B* transcripts were not modified by expression of U7_SKIP (Supp. Fig. S2B), strongly suggesting that the phosphoinositide 5-phosphatase activity observed in cells of the

patient after U7_SKIP expression was due to *OCRL* expression. We concluded that a restoration of normal *OCRL* mRNA after exon skipping with the U7_SKIP construct induced the expression of a functional OCRL-1 protein, restoring the PI(4,5)P2 phosphatase activity in patient's fibroblasts.

Skipping of the Pseudo-Exon 4b Corrects Cellular Phenotypes Linked to OCRL-1 Dysfunction

Alteration of OCRL-1 function in cells from Lowe patients was previously shown to impact on several cellular processes. Early studies on fibroblast pointed to a default in actin dynamic, revealed by shorter actin stress fibers and altered repartition of α-actinin [Suchy and Nussbaum, 2002]. In agreement with our previous work [Montjean et al., 2014], 92% (±8%) of cells from the patient showed abnormal cytoplasmic accumulation of punctuate aggregates of α-actinin, whereas in a control culture very low level of such staining was detected (6% ±0.6) (Fig. 4A). The expression of U7_SKIP, but not of the U7_CTRL, drastically reduced the number of cells presenting this α-actinin punctuate staining (21% ± 3.7), suggesting that upon pseudo-exon 4b skipping and OCRL-1 protein restoration, the intracellular organization of α-actinin was rescued. Recent investigations have shown that late phases of the endocytic process were altered in cells of patients with OCRL-1 mutations [Nández et al., 2014]. In particular, patient's fibroblasts accumulate uncoated clathrin vesicles, which can be visualized by an aggregate staining pattern of the SNX9 protein [Nández et al., 2014], a direct interactor of OCRL-1-linking clathrin-coated pits to polymerized actin. Accordingly, we observed in the culture of the patient fibroblasts a high proportion of cells with a marked punctuated SNX9 pattern (77.1% ± 5.0) in comparison to the control culture (26.4% ± 4.4) (Fig. 4B). The expression of U7_SKIP in fibroblasts of the patient drastically reduced the proportion of cells with a punctuated SNX9 labeling (17% ± 2.4) showing that the skipping of the pseudo-exon 4b restored the correct repartition of SNX9 in these cells.

Several reports have shown that cells lacking OCRL-1 display reduced primary cilium length [Coon et al., 2012; Luo et al., 2012]. Immunolabeling of primary cilium of control or patient fibroblasts were realized (Fig. 4C) and, in accordance with previously published results, a marked reduction of cilium length was observed (3.7μm ± 0.11 vs. 5.2 μm ± 0.13 for control) in the patient cells. Upon specific expression of the U7_SKIP construct, a partial, but significant restoration of primary cilium length was monitored (4.6μm ± 0.08). Overall, we concluded from these observations that U7_SKIP expression mediated the restoration of a significant amount of a functional OCRL-1 protein in fibroblasts of the patient, able to rescue typical cellular defects for Lowe syndrome, that is, accumulations of PI(4,5)P2, α-actinin, and SNX9 aggregates and reduction of primary cilium length.

Discussion

We report here the first Lowe syndrome case caused by a deep intronic mutation in the *OCRL* gene for which an in vitro exon-skipping therapy has been successfully tested. The c.238+4701 A>G mutation created a donor splice site in intron 4 of the *OCRL* gene that was efficiently used with a 3' cryptic acceptor site to trigger the inclusion of a 66-bp intronic sequence in *OCRL* mRNA (pseudo-exon 4b). The mutation has the strongest prediction score for a donor splice site according to the Human Splicing Finder (http://www.umd.be/HSF3/) prediction tool, and our RT-PCR analysis confirmed that most of the patient *OCRL* transcripts contain the pseudo-exon 4b insertion. The presence of an in-frame STOP codon in pseudo-exon 4b is probably responsible for a nonsense-mediated mRNA decay mechanism leading to the overall low level of *OCRL* transcript that we observed in cells of the patient. The reduction in *OCRL* mRNA and the presence of the early STOP codon predicted an absence of the protein, which was confirmed by Western blot. Overall, the genetic characterization of the c.238+4701 A>G; p.Ser80_Gly81ins22*4 *OCRL* mutation, as a loss of function mutation, is in full accordance with the typical clinical signs observed in the patient.

The genetic correction by exon skipping has been successfully tested in numerous in vitro studies to modify mRNA composition of target genes [Veltrop and Aartsma-Rus, 2014], and was pushed forward to clinical trial for gene therapy in a few inherited diseases [Siva et al., 2014; Touznik et al., 2014]. It can therefore be envisaged for potential personalized medicine, providing that its efficiency is demonstrated on individual genetic variations. The diagnosis of c.238+4701A>G mutation in *OCRL* prompted us to evaluate exon skipping as a possible therapy for Lowe syndrome for the following reasons. First, the outcome of the mutation is a pseudo-exon insertion; therefore, exon skipping would restore normal mRNA in cells of the patient. Second, Lowe syndrome being so far associated with a loss of OCRL-1 enzymatic activity, it can be speculated that even a minimal restoration of the protein would raise the phosphoinositide 5-phosphatase activity to a level allowing a rescue of cellular defects. Along these lines, we described in a previous study that residual cellular OCRL-1 PI(4,5)P2 phosphatase activity was associated with the less severe clinical signs [Hichri et al., 2011] among a cohort of patients. It can also be hypothesized that full expression of OCRL-1 at the scale of the kidney may not be mandatory for the correct organ function, because female carrier of *OCRL* mutation are described as asymptomatic, although they probably express variable levels of OCRL-1 activities due to random X-inactivation [Lin et al., 1999]. The U7_SKIP construct was designed to block pseudo-exon 4b incorporation in *OCRL* mRNA. It efficiently induced a decrease in the quantity of mutated *OCRL* transcript together with a rise in total *OCRL* mRNA levels. These results suggest that the U7_SKIP snRNA triggered a shift in *OCRL* splicing, by blocking splicing sites of pseudo-exon 4b and therefore inducing the use of the physiological sites for exons 4 and 5. The recovery of *OCRL* mRNA up to 52% of control cells allowed the synthesis of detectable levels of the protein up to 30%. Although OCRL-1 protein restoration was strong, it was difficult to predict to what extent it could rescue cellular defects associated with the initial loss-of-function of the gene. We thus demonstrated that the restored protein had detectable PI(4,5)P2 phosphatase activity, and was able to significantly reduce the PI(4,5)P2 accumulation detected in fibroblasts of the patient. Noticeably, the level of phosphatase activity restored by exon skipping correlates with the 30% level of OCRL-1 protein detected in treated cells. The characteristic accumulation of PI(4,5)P2 in Lowe patient cells was previously shown to maintain actin polymerization in specific sites such as early invaginations of plasma membranes during the endocytosis process [Nández et al., 2014], or at the cleavage furrow during cytokinesis [Dambournet et al., 2011]. Although still unclear, the pathophysiology of Lowe syndrome relies at cellular level on this generalized dysregulation of actin polymerization and endocytosis, which are associated to abnormal α-actinin and SNX9 distribution [Suchy and Nussbaum, 2002; Nández et al., 2014]. Our results showing a strong restoration of the normal α-actinin and SNX9 staining in fibroblasts treated with U7_SKIP suggest that these main cellular dysfunctions could be corrected by re-expression of the OCRL-1 protein. Of note, U7_SKIP treatment reduced by 78% (from 92% to 21%) the number of cells

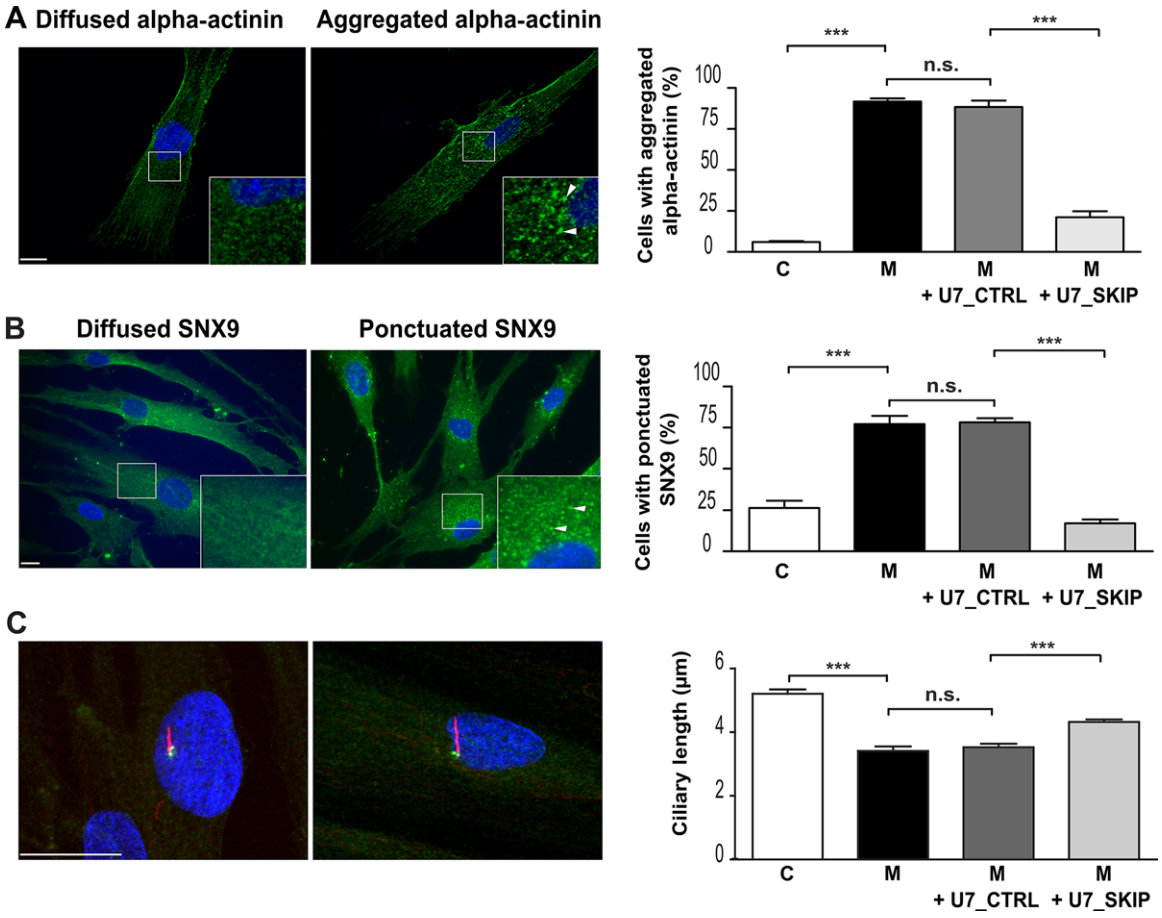

Figure 4. Rescue of cellular phenotypes after exon skipping. **A**: Alpha-actinin staining of cell's typical images showing two different patterns. Images were analyzed to determine the number of cells exhibiting even staining or punctate staining. Histograms represent the average number of cells ± SEM exhibiting an aggregated staining of alpha-actinin in control (C) or patient (M) fibroblasts, or patient fibroblasts transduced with lentiviral vector expressing the U7_CTRL or U7_SKIP construct. *n* = 279 cells for C, 266 for M, 296 for M+U7_CTRL, and 286 for M + U7_SKIP B. SNX9 staining of cell's typical images showing two different patterns. Images were analyzed to determine the number of cells exhibiting even staining or punctate staining. Histograms represent the average number of cells ± SEM exhibiting an aggregated staining of SNX9 in control (C) or patient (M) fibroblasts, or patient fibroblasts transduced with lentiviral vector expressing the U7_CTRL or U7_SKIP construct. *n* = 117 cells for C, 126 for M, 173 for M + U7_CTRL, and 245 for M + U7_SKIP C. Typical images used to monitor primary cilia length: cells are stained with antigamma tubulin (gTub) showing centrosomes as green dots, acetylated tubulin (ac Tub) showing the cilium in red and nuclei (DAPI) in blue on the merged picture. Histograms represent the average primary cilia length ± SEM for control (C) or patient (M) fibroblasts, or patient fibroblasts transduced with lentiviral vector expressing the U7_CTRL or U7_SKIP construct. *n*, 146 cells for C, 193 cells for M, and 193 cells and 288 cells for fibroblasts transduced with lentiviral vector expressing the U7_CTRL and U7_SKIP construct. ANOVA test, $^{***}P < 0.001$. n.s., nonsignificant. Scales bars = 10μm.

showing α-actinin accumulation and by 61% (from 78% to 17%) the number of cells showing SNX9-punctuated staining, whereas only an average of 30% of OCRL-1 was detected in these cells. This surprisingly high efficiency on the restoration of both phenotypes shows that minimal amounts of OCRL-1 could ensure enough PI(4,5)P2 phosphatase activity to regulate actin polymerization and the endocytic process. The restoration of primary cilia growth was milder (24%, from 3.7 to 4.6 μm) and correlates more directly with the level of the restored PI(4,5)P2 content. This indicates a differential sensitivity of the various *OCRL* associated phenotypes relatively to PI(4,5)P2 accumulation. Accordingly, a recent work on the *OCRL*-deficient zebrafish model of Lowe syndrome suggested that the PI(4,5)P2 accumulation-induced kidney defect was more linked to an impaired endocytic pathway [Oltrabella et al., 2015] rather than to a mild primary cilia defect.

To date, trials for gene therapy for several inherited diseases have been launched with various approaches. Among them, manipulations of mRNA composition offer the advantage to aim a restoration of protein levels in a physiological range, without possible overexpression as it will be regulated by the physiological mechanisms of mRNA production. This fine-tuning is of particular interest for correction of *OCRL* mutations as it was also recently reported that a duplication of the gene was associated to autism [Schroer et al., 2012]. An exon-skipping strategy such as the one we developed for the c.238+4701 A>G mutation could restore enough transcript for functional impact without reaching deleterious overexpression. The potential of exon skipping as a therapeutic approach has benefited of recent advances in the delivery of the active molecules to the target organ. Synthetic-modified oligonucleotide such as phosphorothiate were first used and shown to be efficient in vitro and by systemic injection [Aartsma-Rus et al., 2003; Cirak et al., 2011]. They were used in phase III trials for Duchenne myopathy and represent the main therapeutic molecule for mRNA-based therapies [Flanigan et al., 2013], but new chemistry of oligonucleotides

are now proposed [Prakash, 2011] that could in the near future improve their distribution and efficacy when injected systemically. Gene therapy has also been successfully undertaken with viral vectors [Gedicke-Hornung et al., 2013], used to deliver exon-skipping molecules. Antisense sequences fused to U7 snRNA were delivered via viral vectors such as AAV (adeno-associated virus) in animal models [Vulin et al., 2012] and, interestingly, kidney is efficiently reached by these type of vectors even when injected systemically [Zincarelli et al., 2008]. It was also demonstrated that intrarenal arterial administration of AAV2 on mice models leads to highly specific expression of the transgene in the kidney [Chen et al., 2003]. Overall, the conjunction of many recent advances has set a favorable landscape in which one can envisage the delivery of molecules able to modify in vivo a target mRNA in the kidney. Lowe syndrome is a congenital disorder with a progressive renal disease, and in the case of mutations affecting *OCRL* mRNA splicing, an exon-skipping therapy set up after birth could reduce or delay the evolution of the proximal tubule dysfunction. In this context, our demonstration of the efficacy of the U7_SKIP antisense on cellular phenotype of patients' cells is, to our knowledge, the first proof of concept that an inherited kidney disease could benefit from genetic therapy by mRNA manipulation.

Acknowledgments

We thank the family members for their contribution to this study. We thank Professor Ronco for his help. We also thank Delphine Martinez and Joelle Lerale for their precious technical help. We also thank the Association du Syndrome de Lowe for their support, the patient and his family.

Disclosure statement The authors declare no conflict of interest.

Author Contribution

J.R.: design of the work, data acquisition and analysis, draft of the manuscript;R.M.: design of the work, data acquisition and analysis;C.C.: design of the work, data acquisition;M.S.: data acquisition, patient recruitment;G.C.: data acquisition;A.P.: data acquisition;J.B.: data acquisition;F.P.R.: design of the work;B.P.: design of the work, data analysis and manuscript revision;J.L.: design of the work and manuscript revision;O.D.: design of the work, data analysis and manuscript revision;I.M.: manuscript revision; J.F.: design of the work, data analysis, manuscript draft and approval;

References

Aartsma-Rus A. 2003. Therapeutic antisense-induced exon skipping in cultured muscle cells from six different DMD patients. Hum Mol Genet 12:907–914.

Attree O, Olivos IM, Okabe I, Bailey LC, Nelson DL, Lewis RA, McInnes RR, Nussbaum RL. 1992. The Lowe's oculocerebrorenal syndrome gene encodes a protein highly homologous to inositol polyphosphate-5-phosphatase. Nature 358:239–242.

Bernard DJ, Nussbaum RL. 2010. X-inactivation analysis of embryonic lethality in Ocrl wt/-; Inpp5b-/- mice. Mamm Genome 21:186–194.

Bothwell SP, Farber LW, Hoagland A, Nussbaum RL. 2010. Species-specific difference in expression and splice-site choice in Inpp5b, an inositol polyphosphate 5-phosphatase paralogous to the enzyme deficient in Lowe Syndrome. Mamm Genome 21:458–466.

Cavalieri S, Pozzi E, Gatti RA, Brusco A. 2012. Deep-intronic ATM mutation detected by genomic resequencing and corrected in vitro by antisense morpholino oligonucleotide (AMO). Eur J Hum Genet 21:774–778.

Chen S, Agarwal A, Glushakova OY, Jorgensen MS, Salgar SK, Poirier A, Flotte TR, Croker BP, Madsen KM, Atkinson MA, Hauswirth WW, Berns KI, et al. 2003. Gene delivery in renal tubular epithelial cells using recombinant adeno-associated viral vectors. J Am Soc Nephrol 14:947–958.

Cho HY, Lee BH, Choi HJ, Ha IS, Choi Y, Cheong HI. 2008. Renal manifestations of Dent disease and Lowe syndrome. Pediatr Nephrol 23:243–249.

Cirak S, Arechavala-Gomeza V, Guglieri M, Feng L, Torelli S, Anthony K, Abbs S, Garralda ME, Bourke J, Wells DJ, Dickson G, Wood MJA, et al. 2011. Exon skipping and dystrophin restoration in patients with Duchenne muscular dystrophy after systemic phosphorodiamidate morpholino oligomer treatment: an open-label, phase 2, dose-escalation study. Lancet 378:595–605.

Coon BG, Hernandez V, Madhivanan K, Mukherjee D, Hanna CB, Barinaga-Rementeria Ramirez I, Lowe M, Beales PL, Aguilar RC. 2012. The Lowe syndrome protein OCRL1 is involved in primary cilia assembly. Hum Mol Genet 21:1835–1847.

Coutton C, Bidart M, Rendu J, Devillard F, Vieville G, Amblard F, Lopez G, Jouk P-S, Satre V. 2013. 190-kb duplication in 1p36.11 including PIGV and ARID1A genes in a girl with intellectual disability and hexadactyly. Clin Genet 84:596–599.

Dambournet D, Machicoane M, Chesneau L, Sachse M, Rocancourt M, El Marjou A, Formstecher E, Salomon R, Goud B, Echard A. 2011. Rab35 GTPase and OCRL phosphatase remodel lipids and F-actin for successful cytokinesis. Nat Cell Biol 13:981–988.

Di Paolo G, De Camilli P. 2006. Phosphoinositides in cell regulation and membrane dynamics. Nature 443:651–657.

Dominski Z, Kole R. 1993. Restoration of correct splicing in thalassemic pre-mRNA by antisense oligonucleotides. Proc Natl Acad Sci U S A 90:8673–8677.

Erdmann KS, Mao Y, McCrea HJ, Zoncu R, Lee S, Paradise S, Modregger J, Biemesderfer D, Toomre D, De Camilli P. 2007. A role of the Lowe syndrome protein OCRL in early steps of the endocytic pathway. Dev Cell 13:377–390.

Faucherre A, Desbois P, Satre V, Lunardi J, Dorseuil O, Gacon G. 2003. Lowe syndrome protein OCRL1 interacts with Rac GTPase in the trans-Golgi network. Hum Mol Genet 12:2449–2456.

Flanigan KM, Voit T, Rosales XQ, Servais L, Kraus JE, Wardell C, Morgan A, Dorricott S, Nakielny J, Quarcoo N, Liefaard L, Drury T, et al. 2013. Pharmacokinetics and safety of single doses of drisapersen in non-ambulant subjects with Duchenne muscular dystrophy: results of a double-blind randomized clinical trial. Neuromuscul Disord 24:16–24.

Gedicke-Hornung C, Behrens-Gawlik V, Reischmann S, Geertz B, Stimpel D, Weinberger F, Schlossarek S, Précigout G, Braren I, Eschenhagen T, Mearini G, Lorain S, et al. 2013. Rescue of cardiomyopathy through U7snRNA-mediated exon skipping in Mybpc3-targeted knock-in mice. EMBO Mol Med 5:1060–1077.

Goyenvalle A, Vulin A, Fougerousse F, Leturcq F, Kaplan J-C, Garcia L, Danos O. 2004. Rescue of dystrophic muscle through U7 snRNA-mediated exon skipping. Science 306:1796–1799.

Goyenvalle A, Babbs A, van Ommen G-JB, Garcia L, Davies KE. 2009. Enhanced exon-skipping induced by U7 snRNA carrying a splicing silencer sequence: promising tool for DMD therapy. Mol Ther J Am Soc Gene Ther 17:1234–1240.

Goyenvalle A, Davies KE. 2011. Engineering exon-skipping vectors expressing U7 snRNA constructs for Duchenne muscular dystrophy gene therapy. Methods Mol Biol Clifton NJ 709:179–196.

Grieve AG, Daniels RD, Sanchez-Heras E, Hayes MJ, Moss SE, Matter K, Lowe M, Levine TP. 2011. Lowe syndrome protein OCRL1 supports maturation of polarized epithelial cells. PLoS One 6:e24044.

Hichri H, Rendu J, Monnier N, Coutton C, Dorseuil O, Poussou RV, Baujat G, Blanchard A, Nobili F, Ranchin B, Remesy M, Salomon R, et al. 2011. From Lowe syndrome to Dent disease: correlations between mutations of the OCRL1 gene and clinical and biochemical phenotypes. Hum Mutat 32:379–388.

Hoopes RR, Shrimpton AE, Knohl SJ, Hueber P, Hoppe B, Matyus J, Simckes A, Tasic V, Toenshoff B, Suchy SF, Nussbaum RL, Scheinman SJ. 2005. Dent disease with mutations in OCRL1. Am J Hum Genet 76:260–267.

Li P, Zhang J, Fan J, Zhang Y, Hou H. 2014. Development of noninvasive prenatal diagnosis of trisomy 21 by RT-MLPA with a new set of SNP markers. Arch Gynecol Obstet 289:67–73.

Lin T, Lewis RA, Nussbaum RL. 1999. Molecular confirmation of carriers for Lowe syndrome. Ophthalmology 106:119–122.

Loi M. 2006. Lowe syndrome. Orphanet J Rare Dis 1:16.

Lowe C, Terrey M, MacLachlan EA. 1952. Organic-aciduria, decreased renal ammonia production, hydrophthalmos, and mental retardation: a clinical entity. AMA Am J Dis Child 83:164–184.

Lowe M. 2005. Structure and function of the Lowe syndrome protein OCRL1: structure and function of OCRL1. Traffic 6:711–719.

Luo N, Kumar A, Conwell M, Weinreb RN, Anderson R, Sun Y. 2013. Compensatory role of inositol 5-phosphatase INPP5B to OCRL in primary cilia formation in oculocerebrorenal syndrome of Lowe. PLoS One 8:e66727.

Luo N, West CC, Murga-Zamalloa CA, Sun L, Anderson RM, Wells CD, Weinreb RN, Travers JB, Khanna H, Sun Y. 2012. OCRL localizes to the primary cilium: a new role for cilia in Lowe syndrome. Hum Mol Genet 21:3333–3344.

Madhivanan K, Ramadesikan S, Aguilar RC. 2015. Role of Ocrl1 in primary cilia assembly. Int Rev Cell Mol Biol 317:331–347.

McCrea HJ, Paradise S, Tomasini L, Addis M, Melis MA, De Matteis MA, De Camilli P. 2008. All known patient mutations in the ASH-RhoGAP domains of OCRL affect targeting and APPL1 binding. Biochem Biophys Res Commun 369:493–499.

Montjean R, Aoidi R, Desbois P, Rucci J, Trichet M, Salomon R, Rendu J, Faure J, Lunardi J, Gacon G, Billuart P, Dorseuil O. 2014. OCRL-mutated fibroblasts from

patients with Dent-2 disease exhibit INPP5B-independent phenotypic variability relatively to Lowe syndrome cells. Hum Mol Genet 24:994–1006.

Nández R, Balkin DM, Messa M, Liang L, Paradise S, Czapla H, Hein MY, Duncan JS, Mann M, De Camilli P. 2014. A role of OCRL in clathrin-coated pit dynamics and uncoating revealed by studies of Lowe syndrome cells. eLife 3:e02975.

Nussbaum RL, Orrison BM, Jänne PA, Charnas L, Chinault AC. 1997. Physical mapping and genomic structure of the Lowe syndrome gene OCRL1. Hum Genet 99:145–150.

Oltrabella F, Pietka G, Ramirez IB-R, Mironov A, Starborg T, Drummond IA, Hinchliffe KA, Lowe M. 2015. The Lowe syndrome protein OCRL1 is required for endocytosis in the zebrafish pronephric tubule. PLoS Genet 11:e1005058.

Prakash TP. 2011. An overview of sugar-modified oligonucleotides for antisense therapeutics. Chem Biodivers 8:1616–1641.

Recker F, Zaniew M, Böckenhauer D, Miglietti N, Bökenkamp A, Moczulska A, Rogowska-Kalisz A, Laube G, Said-Conti V, Kasap-Demir B, Niemirska A, Litwin M, et al. 2015. Characterization of 28 novel patients expands the mutational and phenotypic spectrum of Lowe syndrome. Pediatr Nephrol Berl Ger 30:931–943.

Rendu J, Brocard J, Denarier E, Monnier N, Piétri-Rouxel F, Beley C, Roux-Buisson N, Gilbert-Dussardier B, Perez MJ, Romero N, Garcia L, Lunardi J, et al. 2013. Exon skipping as a therapeutic strategy applied to an RYR1 mutation with pseudo-exon inclusion causing a severe core myopathy. Hum Gene Ther 24:702–713.

Schroer RJ, Beaudet AL, Shinawi M, Sahoo T, Patel A, Sun Q, Skinner C, Stevenson RE. 2012. Duplication of OCRL and adjacent genes associated with autism but not Lowe syndrome. Am J Med Genet A 158A:2602–2605.

Siva K, Covello G, Denti MA. 2014. Exon-skipping antisense oligonucleotides to correct missplicing in neurogenetic diseases. Nucleic Acid Ther 24:69–86.

Suchy SF, Nussbaum RL. 2002. The deficiency of PIP2 5-phosphatase in Lowe syndrome affects actin polymerization. Am J Hum Genet 71:1420–1427.

Touznik A, Lee JJ, Yokota T. 2014. New developments in exon skipping and splice modulation therapies for neuromuscular diseases. Expert Opin Biol Ther 14:809–819.

Veltrop M, Aartsma-Rus A. 2014. Antisense-mediated exon skipping: taking advantage of a trick from mother nature to treat rare genetic diseases. Exp Cell Res 325: 50–55.

Vicinanza M, Di Campli A, Polishchuk E, Santoro M, Di Tullio G, Godi A, Levtchenko E, De Leo MG, Polishchuk R, Sandoval L, Marzolo M-P, De Matteis MA. 2011. OCRL controls trafficking through early endosomes via PtdIns4,5P_2-dependent regulation of endosomal actin. EMBO J 30:4970–4985.

Vulin A, Barthélémy I, Goyenvalle A, Thibaud J-L, Beley C, Griffith G, Benchaouir R, Hir M le, Unterfinger Y, Lorain S, Dreyfus P, Voit T, et al. 2012. Muscle function recovery in golden retriever muscular dystrophy after AAV1-U7 exon skipping. Mol Ther J Am Soc Gene Ther 20:2120–2133.

Wenk MR, Lucast L, Di Paolo G, Romanelli AJ, Suchy SF, Nussbaum RL, Cline GW, Shulman GI, McMurray W, De Camilli P. 2003. Phosphoinositide profiling in complex lipid mixtures using electrospray ionization mass spectrometry. Nat Biotechnol 21:813–817.

Zhang X, Jefferson AB, Auethavekiat V, Majerus PW. 1998. The protein deficient in Lowe syndrome is a phosphatidylinositol-4,5-bisphosphate 5-phosphatase. Proc Natl Acad Sci U S A 92:4853–4856.

Zhang X, Hartz PA, Philip E, Racusen LC, Majerus PW. 1998. Cell lines from kidney proximal tubules of a patient with Lowe syndrome lack OCRL inositol polyphosphate 5-phosphatase and accumulate phosphatidylinositol 4,5-bisphosphate. J Biol Chem 273:1574–1582.

Zincarelli C, Soltys S, Rengo G, Rabinowitz JE. 2008. Analysis of AAV serotypes 1-9 mediated gene expression and tropism in mice after systemic injection. Mol Ther J Am Soc Gene Ther 16:1073–1080.